

ULRR

Prediction of fast pyrolysis products yields using lignocellulosic compounds and ash contents

Item Type	Article
Authors	Trubetskaya, Anna;Timko, Michael T.;Umeki, Kentaro
Citation	Applied Energy;257, 113897
Publisher	Elsevier
Download date	2026-06-08 17:39:00
Item License	https://creativecommons.org/licenses/by-nc-sa/1.0/
Link to Item	https://hdl.handle.net/10344/8199

Prediction of fast pyrolysis products yields using lignocellulosic compounds and ash contents

Anna Trubetskaya^{a,*}, Michael T Timko^b, Kentaro Umeki^c

^a*School of Engineering and Ryan Institute, National University of Ireland Galway, Galway, Ireland*

^b*Chemical Engineering Department, Worcester Polytechnic Institute, 01609 Worcester, MA, USA*

^c*Division of Energy Science, Luleå University of Technology, 97187, Luleå, Sweden*

Abstract

The effects of lignocellulosic biomass composition on product yields and distributions were studied under high-temperature pyrolysis conditions (800 to 1250°C) in a drop tube reactor. Several types of biomass were studied along with xylan, cellulose, and two types of lignin as model feeds. Among the model feeds, soot yields obtained from lignin pyrolysis were greater than those obtained from cellulose or xylan. Cellulose pyrolysis produced mostly gaseous products, along with small amounts of tars. Impregnation of lignin with alkali metals greatly reduced tar and soot formation, simultaneously increasing the hydrogen content of the syngas product. An empirical model predicted with reasonable accuracy trends in the product yields obtained from pyrolysis of whole biomass samples using data obtained from model feeds composition data and the pyrolysis temperature. Reaction temperature and ash content both have a strong influences on char yield, whereas gas yields were mostly affected by the reaction temperature.

*Corresponding author. anna.trubetskaya@nuigalway.ie

Keywords: fast pyrolysis, lignin, potassium, residence time, modeling

1. Introduction

Entrained flow gasification (EFG) combined with catalytic syngas upgrading has potential for large-scale production of second-generation biofuels leading to energy sector decarbonization [1]. Gasification involves conversion of lignocellulosic feedstocks into synthesis gas (syngas), which can be used as a feed to produce chemicals (methanol, ammonia) or liquid transport fuels (synthetic natural gas, Fischer-Tropsch fuels) [2]. Chemically, gasification combines drying, devolatilization, and partial oxidation processes. The heat required for the endothermic reactions during devolatilization and gasification is generated by exothermic partial oxidation [3]. Careful balancing of partial oxidation and gasification reactions can result in an overall energy balance which is close to thermoneutral, thus eliminating the need for heat management that can negatively impact energy yields.

The EFG process achieves high carbon conversion by exposing biomass to temperatures ranging from 1100 to 1500°C for residence times less than a few seconds. While the rapid reactions are beneficial for highly intensified chemical processes, these conditions also result in soot formation. Tar is composed of organic compounds, including aromatics and polycyclic aromatic hydrocarbons (PAHs). PAHs are stable at high temperatures and eventually form soot particles which can reduce process efficiency due to increased bulk viscosity, decreased cold gas efficiency, and deposition of particulate matter downstream. Char, the unreacted biomass residue, is also problematic for similar reasons. The thermal profile and residence time in

the gasifier both play important roles in determining char and soot yields, size, and nanostructure [4, 5]. In addition, increasing residence time promotes agglomeration of primary soot spherules into larger particles which rapidly deposit downstream, thereby hindering operation and requiring frequent removal. Reducing soot, char, and soot formation can increase overall process efficiency, improve the outlet syngas quality and composition, and benefit the economic performance and reliability of gasification plants.

Fast pyrolysis at high temperatures and heating rates is the initial step of the biomass gasification. The pyrolysis literature contains only a few examples of models that can predict char and gas yields, which means that current understanding is based primarily on empirical studies [6, 7]. Most parametric studies indicate that char formation in the pyrolysis is determined by a combination of factors, which include fuel particle size, feedstock type, residence time, and heat treatment temperature [5, 8–10]. Moreover, feedstock composition strongly affects pyrolysis reactivity and product yields [5]. Ash content, especially alkali and alkaline earth metals (AAEM), is known to act catalytically in pyrolysis reactions [11]. Most of the existing biomass pyrolysis models [12–15] that describe both the devolatilization product composition and yields (light gases, tar and char) are mainly valid for low-ash fuels (hardwood, softwood); whereas considerably less work has been carried out with herbaceous lignocellulosic materials, which have comparatively greater ash content.

Several attempts at development of empirical models for char prediction appear in the literature [16–20]. An empirical model proposed by Trubet-

skaya et al. [19] for herbaceous char yields exhibited significant differences between predictions and measurements. The discrepancy between experimental data and model predictions was attributed to interactions between potassium, other remaining alkali metals, and the carbonaceous char matrix which were not considered during the model development and thus, indicated the importance of inorganic matter on pyrolysis. Moreover, the model proposed by Trubetskaya et al. [19] did not include the influence of lignocellulosic composition on the product yield and composition. However, xylan pyrolysis results in a lower char yield and greater CO₂ reactivity than does pyrolysis of extractives, lignin, or monolignols, a result that indicates the importance of feedstock composition on the product yields and distribution [21]. Along similar lines, Couhert et al. attempted to model pyrolysis gas yields based on weight fraction additivity law using the yields obtained from isolated cellulose, xylan, and lignin feeds to predict the yields observed for pyrolysis of biomass sample of known composition [22, 23]. However, the model predictions deviated significantly from the experimental, suggesting that more sophisticated models may be required to capture observed trends. Specifically, Couhert et al. suggested that the accuracy of future models might be improved by including the effects of heat and mass transfer and terms to describe interactions between biomass components.

The aim of the present study was to evaluate the performance of empirical models to predict char and gas yields from biomass pyrolysis. The specific objectives were to: (1) measure char and gas yields obtained from high-temperature fast pyrolysis of several representative biomass components, including two types of lignin, cellulose, and xylan, and (2) develop empirical

models to relate char and gas yields obtained for the wood and herbaceous biomass to their composition and reactor temperature, using data from the model feeds as the basis of the prediction. **Because char and gas yields depend on feedstock properties, a basic study of fast pyrolysis using isolated biomass components was performed to provide generalizable data for model development. Because pyrolysis performance is highly dependent on reactor conditions, experiments were performed in a well characterized drop tube reactor system to permit model validation. Gas and solid product yields were measured and compared with the predicted solid product yields using simple empirical models. In addition, soot yields were measured, but not modeled. The results from this study provide an empirical guide for gasifier design and indicate the relative importance of composition and reactor conditions on soot yields for future experimental and model development efforts.**

2. Materials and methods

The effects of lignocellulosic compounds and potassium on the product yields and composition were investigated in a drop tube reactor (DTR) as described previously [5]. Two types of organosolv lignin, one obtained from softwood and the other from wheat straw (purity > 94 %), were provided by BOC Sciences. Cellulose Avicel[®] (purity > 99.9 %) and xylan from beechwood (purity > 90 %) were purchased from Sigma-Aldrich. The purity of xylan was increased from 90 % to 96.6 % using a three step procedure involving strong alkali treatment, bleaching, and acetylation. **The lignocellulosic**

compounds were sieved to a particle size fraction of 0.08-0.15 mm. The lignocellulosic compounds were reacted in the DTR at temperatures of 800-1250°C. The effect of potassium on the product yield and composition was investigated by impregnating wheat straw lignin with potassium nitrate. Therefore, wheat straw lignin was impregnated with an aqueous solution of KNO_3 (Alfa Aesar, purity > 99%), whereby 2.5 mg KNO_3 was diluted in deionized water and added to 50 mg lignin. The K content of the impregnated lignin was similar to that previously reported for wheat straw (1.9 %, db) [24]. Unlike use of carbonate salts, the use of nitrates does not impact the carbon balance, and nitrate volatilize during heat up, leaving negligible residue [25]. Based on the experimental results, a model was developed to estimate the char and soot yields from pyrolysis of biomass at conditions relevant to entrained-flow gasification. The model was validated using the product yields of pinewood, beechwood, wheat straw and alfalfa straw and literature results [24, 36].

2.1. Fast pyrolysis in drop tube reactor

The lignocellulosic compounds were reacted at three particle residence times (800°C: 4.7, 6.9, 13.8 s; 1000°C: 3.9, 5.8, 11.6 s; 1250°C: 3.3, 4.8, 9.7 s) in a laminar drop tube reactor. The DTR setup was described in detail by Trubetskaya et al. [5] and shown in Figure 1. The lignocellulosic feed was rapidly heated to reaction temperature after introduction to the reactor. The biomass feed rate was 0.2 g min^{-1} and a total of $\approx 5 \text{ g}$ of biomass were fed in each experiment. Both primary (0.181 min^{-1} measured at 20°C and 101.3 kPa) and secondary (4.81 min^{-1} measured at 20°C and 101.3 kPa) feed

gases were N_2 . The residence time of fuel particles was calculated based on the size of reactor diameter and the total nitrogen flow, taking into account density changes during pyrolysis [17].

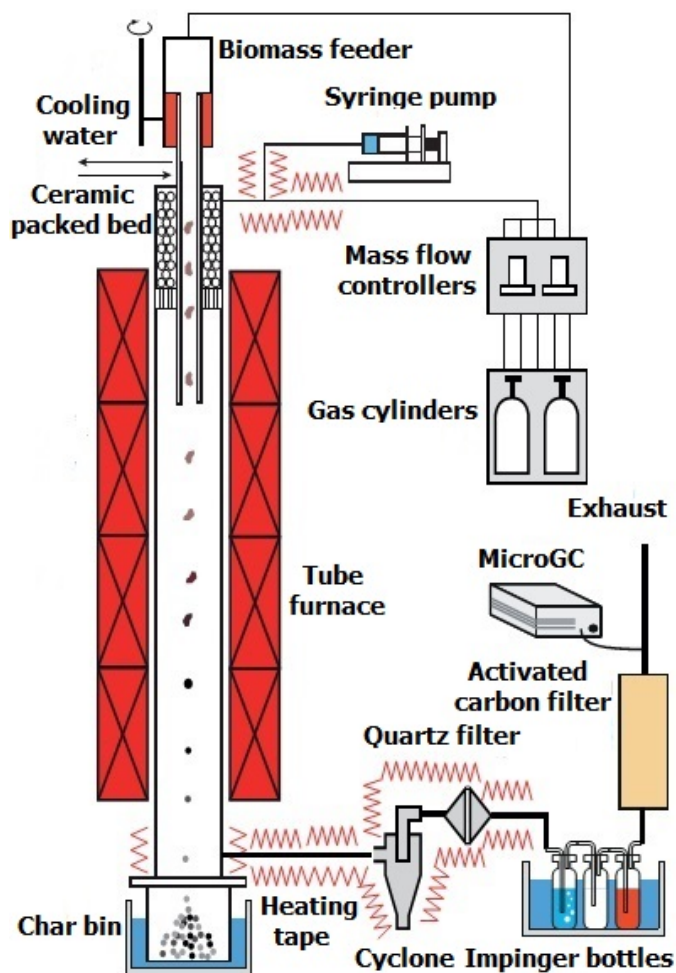


Figure 1: Schematic view of the drop tube reactor at Luleå University of Technology.

The residence time was varied by using different reactor lengths (1.06 and 2.12 m), while the flow rate of feed gases was kept constant. Reaction products were separated into coarse particles (mainly char and fly ashes), fine

particles (mainly soot and ash aerosols), tars, and permanent gases. Soot particles were removed using a cyclone (cut size $2.5\ \mu\text{m}$) followed by a quartz filter (QM-A, 50 mm diameter, $2.2\ \mu\text{m}$ pore size, Whatman, GE Healthcare Life Science). The tars from the product gas flow were collected in three impingers in series; each impinger was filled with 30 ml of methanol (HiPer-Solv CHROMANORM[®], purity $> 99.8\%$). The temperature of methanol was kept at -50°C using a cooling bath Proline Edition X (LAUDA Dr. R. Wobser GmbH, Germany).

2.2. Pyrolysis product characterization

Solid residue characterization. **Solid products were categorized as char, soot, and coke. Char and soot were collected in a char bin and on a filter, respectively. Char is the fraction of non-devolatilized solid present in the initial biomass, consisting mainly of carbon and ash. Coke, the carbonaceous material deposited on the reactor walls, was quantified after each experiment by measurement of the concentration of CO_2 during oxidation.**

Elemental analysis. Elemental analysis was performed on the instrument 2400 CHNS/O Series II (PerkinElmer, UK), **according to the procedure described in ASTM D5373-02.** Acetanilide was used as a reference standard. The tests were repeated in triplicate.

Proximate analysis. **The proximate analysis was conducted to determine the contents of moisture, ash, volatiles, and fixed carbon according to the procedures described in ASTM D2216-19, ASTM**

D1102-84, ASTM D3175-11, and ASTM D3172-13. The high heating value was determined by the bomb calorimetry (IKA C-200), according to the procedure described in ASTM D2015-95.

Ash compositional analysis. The ash compositional analysis was performed using ICP-OES, following in ASTM D6349-13. Prior to each analysis, the biomass sample was heated from room temperature to 550°C using a 10°C min⁻¹ ramp and held at the final temperature for 7 h.

Thermogravimetric analysis. The ash content of char and soot samples was determined using a thermogravimetric analyzer (TGA, Mettler-Toledo) by loading 3 mg of sample in an alumina crucible and heating it from 30 to 700°C in air and at a constant heating rate of 10°C min⁻¹. Ash content was determined as the residual mass remaining after the sample had been heated to 700°C.

3. Results and Discussion

3.1. Model compound characterization

The relationship between the structure of model compounds and their depolymerization behavior has not been widely investigated. A primary objective of this study was to examine the effects of composition on pyrolysis product yields. To this end, cellulose, xylan extracted from beechwood, and two types of lignin were obtained and characterized. Two lignin types were studied as lignin varies more from source to source than either cellulose or xylan.

Table 1: **Proximate, ultimate and ash compositional analyses of cellulose, xylan from beechwood (xylan), lignin from softwood, lignin from wheat straw, pinewood, beechwood, wheat straw, and alfalfa straw.**

	Cellulose	Xylan from beechwood	Lignin from softwood	Lignin from wheat straw	Pinewood	Beechwood	Wheat straw	Alfalfa straw
Proximate and ultimate analysis (% on dry basis)								
Moisture ^a	6	6	4.1	3.8	5.1	4.5	5.5	5.2
Ash (550°C)	0.3	3.7	1.3	3.6	0.3	1.4	4.1	7.4
Volatiles	94.9	81.6	67.3	66.3	86.6	79.4	77.5	75.9
Fixed carbon	4.8	14.7	31.4	30.1	13.1	19.2	18.4	16.7
HHV ^b	18	14	26.4	26.7	21.6	20.2	18.8	19.7
LHV ^b	16.1	12.2	24.9	25.2	20.2	19	17.5	16.9
C	42.3	39.6	59.9	61.1	53.1	50.7	46.6	42.5
H	6.3	6	5.5	5.6	6.5	5.9	6.1	6.7
O	50.9	52.3	31.9	28.2	40	41.9	42.5	43.1
N	0.3	0.2	1.2	0.8	0.06	0.13	0.6	0.3
S		0.1	0.8	0.1	<0.01	0.02	0.1	0.03
Ash compositional analysis (mg kg ⁻¹ dry basis)								
Cl		0.01	0.5	0.03	0.01	0.02	0.1	0.5
Al		10	100	300	10	10	150	600
Ca		5700	250	200	600	2000	2500	12900
Fe		1500	600	1400	20	10	200	
K		180	80	270	200	3600	11000	28000
Mg		80	<30	40	100	600	750	1400
Na		19200	4100	6800	30	100	150	1000
P		150	30	30	6	150	550	1900
Si		3	900	4000	50	200	8500	2000
Ti		100	50	100	2	8	10	30

^a wt. % (as received) ^b in MJ kg⁻¹

Both lignin samples were characterized as guaiacyl-syringyl GS type [26]. However, previous study showed that lignin from softwood contains the greater fraction of carbohydrates than lignin from wheat straw [4]. Moreover, lignin from wheat straw has one additional structural unit of p-hydroxyphenolic

origin [27].

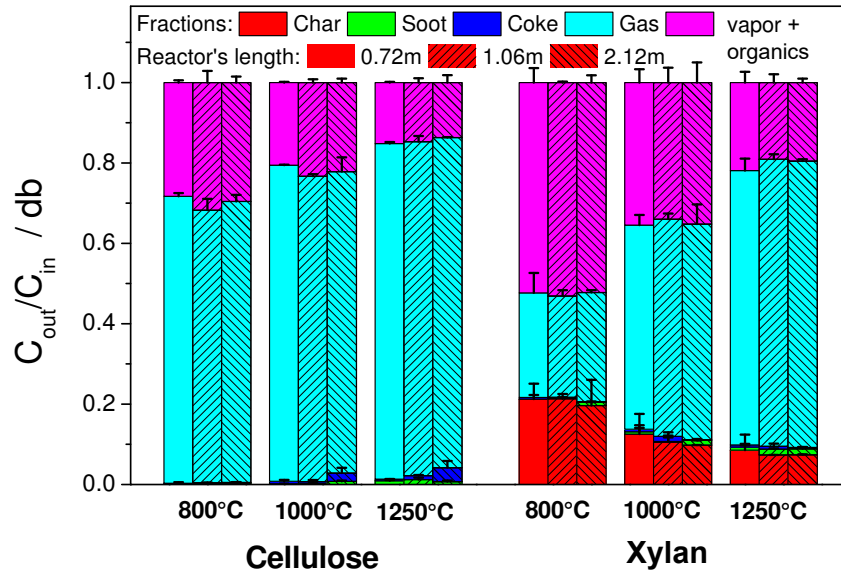
Understanding of elemental composition is important in the predictive modeling of product yields. Table 1 provides ultimate and proximate analysis data obtained for the lignocellulosic feeds. In addition, previous reports suggest that alkali salts play catalytic roles during pyrolysis [28, 29]. Lignin from wheat straw was rich in Na, Si and Fe, whereas lignin from softwood contained less Na. Several studies [30, 31] reported that potassium catalyzes char production, promoting faster devolatilization rates and suppressing tar formation. However, both lignin samples contained low concentrations of K, consistent with previous reports on lignin obtained from the organosolv process [32]. High amounts of silica in both lignin samples were likely introduced during lignin transportation and storage [33]. The high sodium content in softwood and wheat straw lignin samples was related to the remaining Na^+ ions after organosolv extraction [34, 35].

Feedstock selection for the model validation was based on the differences in the ash composition and plant cell compounds (cellulose, hemicellulose, lignin, extractives), as shown in the supplemental material (Table S-3). The wood samples are low in ash, with slightly greater potassium and calcium content in beechwood than in pinewood. Wheat straw and alfalfa straw are rich in silicon and alkali (K, Ca, Na), as shown in Table 1.

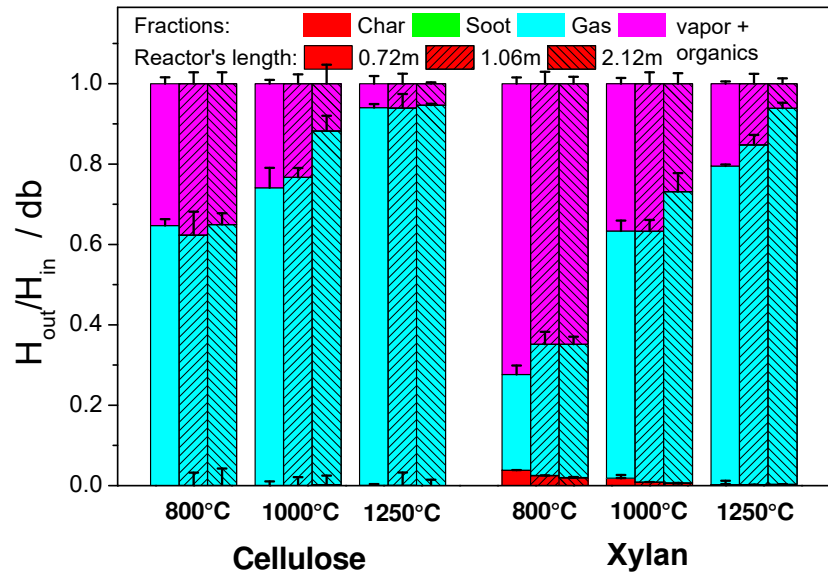
3.2. Carbon and hydrogen balances

Figures 2-3 provide product distribution data obtained from pyrolysis of lignocellulosic compounds, as determined by recovery of solid residues (char, soot, coke) and major gaseous products (CO_2 , H_2 , CO , CH_4 , C_2H_4 , C_2H_2 ,

C_2H_6 , C_3H_8). Water, vapor, tars, and large hydrocarbon yields (**organics + vapor**) were not measured directly, instead estimated by gravimetric differences. Carbon and hydrogen balance data provided in Figures 2-3 are averages of at least two measurements. Cellulose pyrolysis yielded mainly gaseous products, along with small amounts of soot, whereas pyrolysis of xylan and lignin yielded more tar and solid residues than gas.

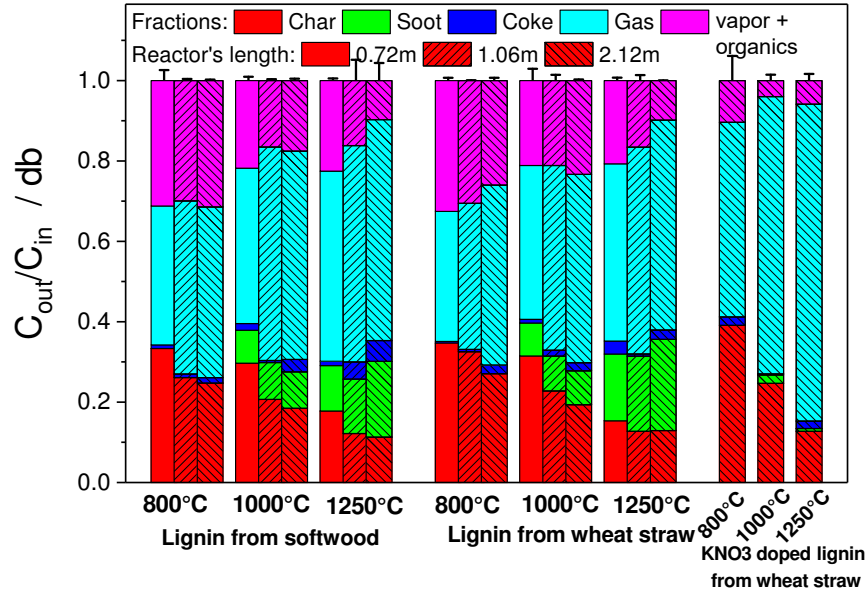


2(a): Carbon distribution

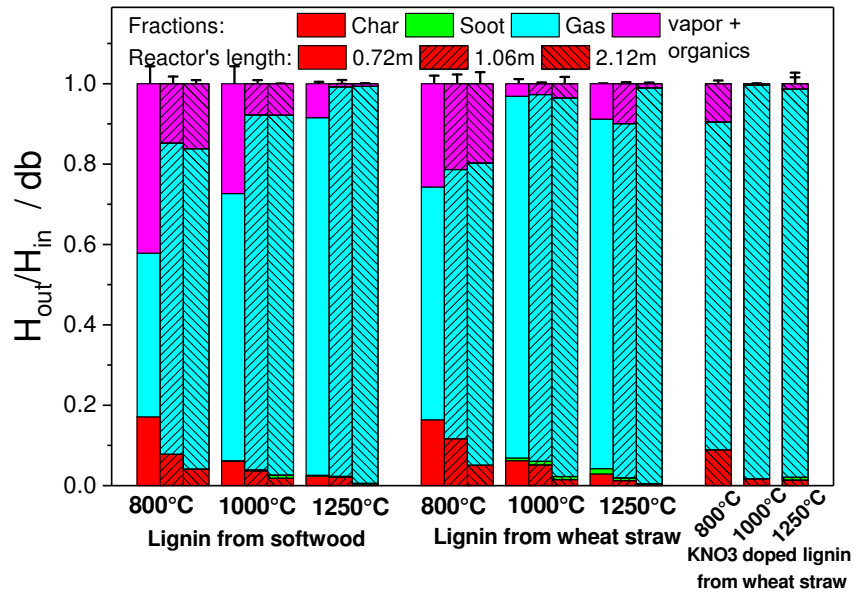


2(b): Hydrogen distribution

Figure 2: Carbon and hydrogen distribution of cellulose and xylan from beechwood reacted at 800, 1000, and 1250°C in the drop tube reactor.



3(a): Carbon distribution



3(b): Hydrogen distribution

Figure 3: Carbon and hydrogen distribution of lignin from softwood, lignin from wheat straw and doped lignin from wheat straw, reacted at 800, 1000, and 1250°C in the drop tube reactor.

Consistent with results reported by Zhou et al. [37] cellulose pyrolysis yielded the most gas, lignin produced the least amount of gas, and xylan produced the most tar. Similar trends in product distributions have been reported using thermogravimetric analysis [38–41]. The majority of hydrogen (> 60 %) was found in the form of gaseous products for pyrolysis of cellulose and both lignin samples, whereas the majority of the hydrogen produced from xylan pyrolysis was contained in the water, tar, and large hydrocarbon products. Similar product distributions were observed for pyrolysis of the two lignin types. The relative gas yields obtained from lignin and cellulose pyrolysis may be attributed to differences in the chemical structures of the feeds.

Lignin is a thermally stable, highly branched heteropolymer consisting of cross-linked aromatic rings with various side chains [42]. Lignin pyrolysis produced the most solid residue, which is consistent with the fixed carbon and ash content of the sample, as shown in Table 1. Cellulose is a linear glucose homopolymer that is less thermally stable than lignin, and its pyrolysis yields more gas products than do other lignocellulosic components [43]. Trends in gas yields were also consistent with elemental analysis of char samples, as shown in the supplemental material (Figure S-1). By focusing on a single feed, Figure 3 provides information on the effects of pyrolysis conditions on product yields. For a given feed, increasing pyrolysis temperature decreases tar formation and increases the hydrogen content of the gaseous products.

Irrespective of the feed, increasing the pyrolysis temperature from 800 to 1250°C increased the hydrogen content of the gas product. Increasing temperature decreased the char, tar, and large hydrocarbon yields obtained

from xylan and lignin, while increasing the gas and soot yields - especially for lignin.

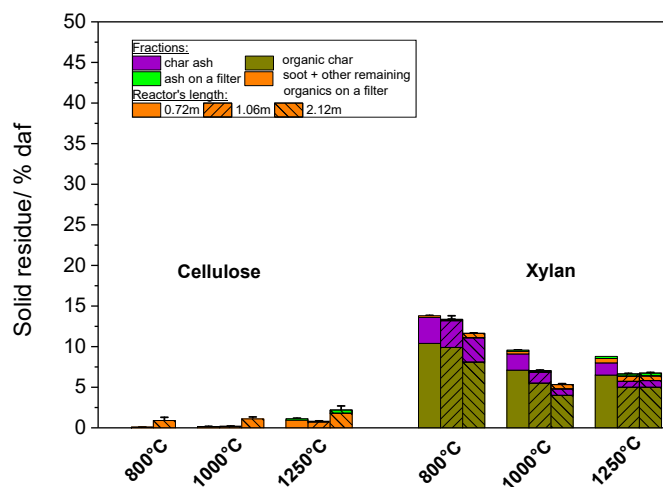
Figures 2-3 indicate differences in the product distributions obtained from pyrolysis of isolated lignocellulosic components compared with whole biomass, consistent with previous reports [5]. Yu et al. suggested that interaction of chemical reactions with finite heat and mass transfer rates as the most likely reason for the different behavior of biomass compared with its isolated constituents [36]. However, in addition to heat and mass transfer through the porous biomass structure, the inorganic content of isolated lignocellulosic components is significantly less than that contained in wood and herbaceous biomass and the catalytic effect of ash may be an important effect to include in empirical pyrolysis models. To examine the effect of alkali content more closely, KNO_3 doped wheat straw lignin was pyrolyzed for direct comparison with the original sample. The advantage of KNO_3 doping is that it varies the concentration of alkali catalysts without altering the pore structure and thereby should not influence heat and mass transfer rates. Increasing the K content of the lignin increased the observed char yield, whereas the soot and tar yields decreased. Moreover, the gas product obtained from pyrolysis of the doped lignin was $> 90\%$ hydrogen, with depressed yields of tar, char and soot, consistent with the previous results reported by Umeki et al. [29], as discussed below. The results of the KNO_3 doping study clearly establish that alkali content must be included in any meaningful model of lignin pyrolysis.

3.3. Soot and char yields

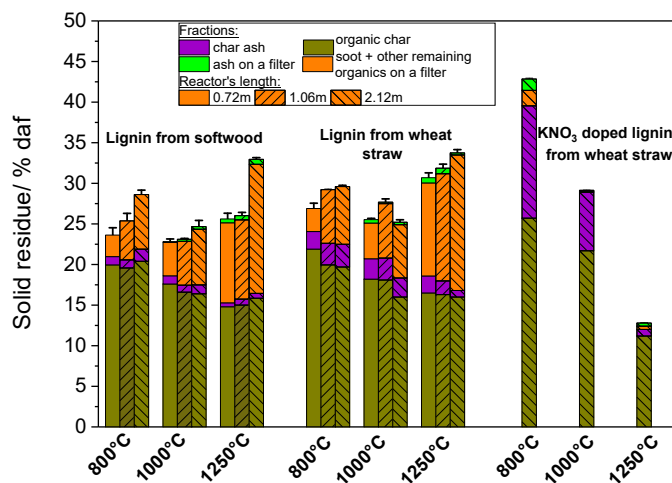
Figure 4 provides soot and char yields, showing that soot yields obtained from pyrolysis of isolated lignocellulosic components were greatest at 1250°C, whereas the char yields decrease with increasing pyrolysis temperature. Lignin pyrolysis yielded the most soot on dry ash free basis (daf), likely attributable to the generation of PAH precursors and ultimately soot from the phenolic components of lignin [44, 45]. Consistent with this explanation, previous studies reported that a significant fraction of aromatic tars and soot formed from lignin pyrolysis is composed of guaiacol and syringol-type units [46–48].

Similar soot yields were obtained from the two different lignin types, as the soot yield obtained from softwood lignin 15.9% wt. daf and from wheat straw lignin it was 16.7% wt. daf at 1250°C. The lignin types exhibited minor differences in soot yield despite different alkali content (i.e. Na⁺), potentially indicating that Na⁺ content plays a secondary role, whereas K⁺ plays a primary one. This might be due to differences in a bonding of Na⁺ or K⁺ ions to the organic structure of lignin [29]. K⁺ ions are intimately bonded within the lignin structure, whereas Na⁺ ions are added to the lignin structure during the organosolv pretreatment, which may contribute to reduced reactivity during pyrolysis. Pyrolysis of cellulose and xylan yielded less soot than lignin. As a general trend, char yield obtained from lignin and xylan decreased with increasing temperature, as shown in Figure 4. Cellulose and xylan pyrolysis generates oxygenated species such as levoglucosan and other anhydrosugars derived from holocelluloses that are precursors of light aromatic compounds that form soot only at greater temperatures than

studied here [49–51]. Char yields obtained from cellulose pyrolysis were less than estimated detection limits (< 0.005 g) in the temperature range from 800 to 1250°C.



4(a): Cellulose and xylan



4(b): Lignin from softwood, from wheat straw and doped lignin

Figure 4: Soot and char yields (wt. % relative to the original lignocellulosic compound) of cellulose, xylan, lignin from **softwood**, and lignin from wheat straw reacted at three different residence times and at 800-1250°C. Additional experiments were done using KNO₃ doped lignin from wheat straw only at one residence time (2.12 m-length reactor). The total yield of soot and char is separated in ash and organic fractions. The error bars characterize the deviations between the total yields of the char and soot.

Ross et al. [52] stated that soot obtained from wood pyrolysis is rich in PAHs, presumably formed via the hydrogen-abstraction-carbon-addition mechanism from acetylene precursors. Consistent with this mechanism, C_2H_2 yields decreased with increasing temperature, whereas soot yields increased. Char yields obtained from lignin and xylan pyrolysis decreased only slightly with increasing residence time. Low heating rates promote high char yields due to finite intra-particle mass transfer rates, leading to secondary reactions that form heavier compounds and char [53]. On the other hand, rapid heating rates, as studied here, lead to rapid volatilization, pressure build-up within the particles, and subsequent evaporation, all of which tend to depress char yields [54].

The results shown in Figure 4 indicate that heat treatment temperature influences char yield more than residence time, possibly due to rapid cracking rates at high heating rates, similar to the findings of Hajaligol et al. [55, 56]. Figure 4 indicates that pyrolysis of potassium-impregnation wheat straw lignin resulted in greater char yields than the non-treated lignin samples at temperatures $> 1000^\circ C$, potentially attributable to potassium-catalyzed repolymerization and cross-linking reactions [57]. In comparison, potassium-impregnated reduced soot yields obtained from lignin, consistent with alkali inhibition of the formation of precursors to PAHs, similar to previous results reported by Umeki et al. [29].

Primary pyrolysis reactions form free radicals intermediates due to cracking of biomass organic constituents [58]. Similarly, potassium rich wheat straw contains greater concentrations of radicals than does ash lean wood, as shown previously [59]. These radicals can recombine to form stable PAHs

structures within the char matrix. The PAH molecules contain delocalized unpaired carbon-centered π -electrons and aliphatic radicals. **The formation of potassium-carbon bonds, such as in the potassium impregnated lignin, could weaken carbon-carbon bonds in aromatic rings and thereby facilitate bond breaking at high temperatures, leading to the low soot yields [60–64].**

3.4. Modeling of product yields

Simple models of char and gas yields are potentially valuable for identifying the relative importance of key variables and guiding future experiments and development of mechanistic models. Previous work by Couhert et al. [23] showed that pyrolysis product yields could not be predicted accurately using a simple additivity law based on the yields of the isolated components, attributing the discrepancy to interactions between chemical reaction rates and heat and mass transfer. Alternative explanations include either interaction between the lignocellulosic components or the influence of ash, neither of which Couhert et al. [23] included explicitly in their model. Specifically in these previous efforts [22, 23] a model of the form of equation 1 was adopted, as shown in Table 2. In equation 1, y is the product yield obtained from pyrolysis of the isolated lignocellulosic compound and γ is the mass fraction of lignocellulosic compounds in the biomass, as shown in the supplemental material (Table S-1 and Table S-2). Inorganic components were considered to be non-reactive, contributing only to the mass of the final char product [65]. A_1 - A_3 in equation 1 are empirical fitting coefficients.

Table 2: The experimental data fitting to predict char and gas yields using a different set of empirical fitting parameters.

Model	Equation	Product	Par. 1	Par. 2	Par. 3	Par. 4	Par. 5	R ² , %
1	$\gamma = A_1 \cdot \gamma_{cel} \cdot y_{cel} + A_2 \cdot \gamma_{xyl} \cdot y_{xyl} + A_3 \cdot \gamma_{lig} \cdot y_{lig}$ (1)	char	-4.5	0.7	1			80
2	$\gamma = B_1 \cdot ((y_{cel} \cdot \gamma_{cel})^{B_2} + (\gamma_{xyl} \cdot y_{xyl})^{B_3} + (y_{lig} \cdot \gamma_{lig})^{B_4}) \cdot \gamma_{ash}^{B_5}$ (2)	char	2.1	1	2.8	2.4	0.8	95
3	$\gamma = C_1 \cdot (y_{cel} \cdot \gamma_{cel} + \gamma_{xyl} \cdot y_{xyl} + y_{lig} \cdot \gamma_{lig})^{C_2} \cdot \gamma_{ash}^{C_3}$ (3)	char	2.1	0.6		0.3		95
4	$\gamma = D_1 \cdot (y_{cel} \cdot \gamma_{cel} + \gamma_{xyl} \cdot y_{xyl} + y_{lig} \cdot \gamma_{lig})^{D_2} \cdot \gamma_{ash}^{D_3} \cdot T_{reac}^{D_4}$ (4)	char	0.7	0.9		1.1	0.9	96
		gas	0.07	-0.28		-0.04	0.9	99
		CH ₄	$6.3 \cdot 10^7$	1		0.06	-1.5	92
		CO	$3.3 \cdot 10^{-8}$	1		-0.02	2.48	99
		CO ₂	$1.9 \cdot 10^8$	$1 \cdot 10^{-4}$		$1 \cdot 10^{-3}$	-2.2	98
5	$\gamma = (E_1 \cdot y_{cel} \cdot \gamma_{cel} + E_2 \cdot \gamma_{xyl} \cdot y_{xyl} + E_3 \cdot y_{lig} \cdot \gamma_{lig}) \cdot \gamma_{ash}^{E_4} \cdot T_{reac}^{E_5}$ (5)	H ₂	$4.6 \cdot 10^{-10}$	1.1		$3 \cdot 10^{-3}$	2.6	98
		char	-59724	5449	13195	0.5	-0.7	97
		gas	$4 \cdot 10^{-6}$	$1.1 \cdot 10^{-5}$	0.4	0.2	0.9	96
		CH ₄	$1.1 \cdot 10^{15}$	$1.3 \cdot 10^{15}$	$1.5 \cdot 10^{-4}$	-0.1	1.3	95
		CO	$1.1 \cdot 10^{-6}$	$2 \cdot 10^{-4}$	$1.5 \cdot 10^{-4}$	-0.1	1.4	98
CO ₂	$1.3 \cdot 10^8$	$1.2 \cdot 10^8$	$4.2 \cdot 10^7$	0.2	-2.3	98		
H ₂	$3.7 \cdot 10^{-6}$	$-4.2 \cdot 10^{-6}$	$1.8 \cdot 10^{-6}$	0.1	1.6	98		

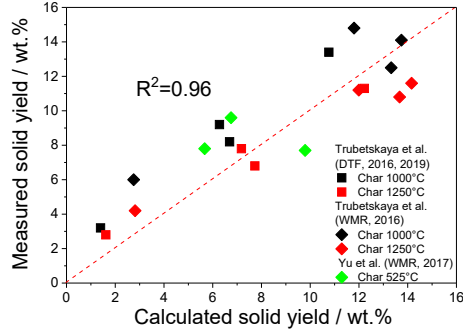
To generalize beyond the current data set, data from the study by Yu et al. [36] - collected under similar conditions to those used in the current study - were included for parameter regression. Values of the A_1 , A_2 , and A_3 parameters were then determined by multiple linear regression. The best fit of the present experimental data [5, 21] obtained using model 1 resulted in $R^2 < 0.8$, with significant scatter. The poor quality of the fits obtained from model 1 indicated a need to expand the model. Based on trends observed in the current data set and in the literature [19, 21], additional parameters were considered to capture the influence of inorganic composition of the feed and reaction temperature on product yields, resulting in a family of models (equations 2-5 in Table 2) for systematic testing. In particular, including

an explicit reaction temperature term may be required for empirically capture the effects of biomass interaction, finite transport rates, and secondary reactions on observed product yields; although models based on yields obtained for the isolated components already contain an implicit temperature dependence, capturing the effects of biomass interactions, transport, and secondary reactions may require an additional, explicit temperature-dependent term. Several different empirical approaches were considered for the effects of biomass composition, as shown in the different forms used in models 2-5.

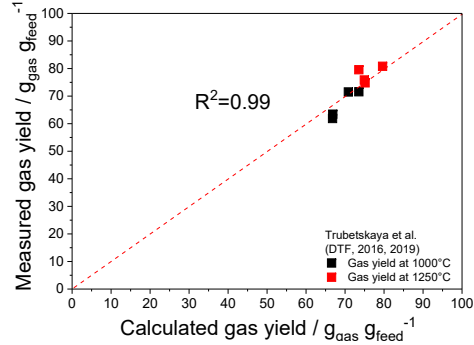
Throughout the modeling exercise, the intention was identification of forms capable of matching available data, with the realization that incomplete models could provide nearly as much value as more accurate ones. In an empirical model, the need for additional parameters must be balanced with the risk of overfitting. To reduce the risk of overfitting, addition of new parameters was always balanced by the observed improvement in fit, in accordance with the precepts of information theory [66].

As in model 1, models 2-5 neglect the effects of extractives and the only effect of ash was included. Of the five models, models 1-3 were applied only to char yield predictions; models 4-5 were used for char predictions and, by using different values for the fitting parameters, total gas yield, and individual gas yields of H_2 , CO , CH_4 , and CO_2 . Soot was excluded from the present study given the lack of comparison data in the literature. Focusing first on char, including terms intended to capture interactions between the various components and the effect of ash - as was done in models 2-3 - improved the correlation constant from 0.80 to 0.95. The superior performance of models 2-3 compared with model 1 is consistent with ash playing a key catalytic role

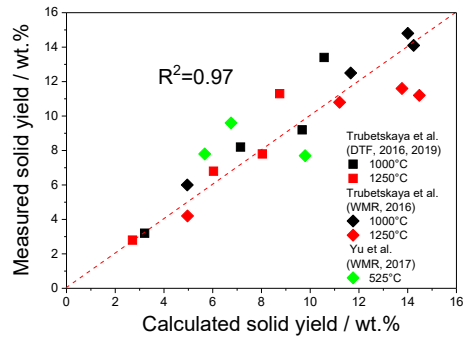
in char formation.



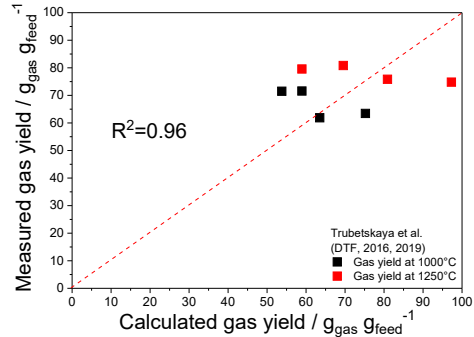
5(a): Parity plot of biomass char yields based on model 4



5(b): Parity plot of biomass gas yields based on model 4



5(c): Parity plot of biomass char yields based on model 5



5(d): Parity plot of biomass gas yields based on model 5

Figure 5: Parity plot of the predicted and observed values of char and gas yields from biomass pyrolysis in the wire mesh and drop tube reactors based on models 4 and 5 using the experimental data from present and previous studies [5, 24, 36].

The effect of additional parameters alone cannot explain the improved performance since model3 and model1 both rely on 3 fitting parameters. Furthermore, comparison of model3 with model2 suggests that combining contributions from the different biomass components can be an effective ap-

proach for reducing the number of required parameters without loss of accuracy. Along the same lines, including a term to capture reaction temperature in models 4-5 resulted in correlation constants of 0.96 and 0.97, respectively. Figure 5 contains parity plots of the predictions of char yields obtained from models 4 (Figure 5(a)) and 5 (Figure 5(c)) with experimental values. In both cases, the model predicts with about 10% accuracy trends in char yields spanning more than an order of magnitude.

Models 1-3 were applied to gas phase data, with resulting correlation coefficients < 0.80 and considerable scatter. Based on these observations, gas phase yields cannot be predicted with accuracy from yields obtained from the isolated biomass components alone. In comparison, including explicit temperature terms - as is done in models 4 and 5 - leads to acceptable predictions of gas product yields. **Models 4-5 were used for predicting total gas yield and the individual yields of the major gases: CH₄, CO, CO₂ and H₂.** The resulting regression parameters are provided in Table 1 and representative parity plots are provided in Figure 5, with more detail in the supplemental material (Figures S-7 and S-8). For both models and for all gases, the quality of fit for the gaseous product yields is acceptable for most applications ($R^2 > 0.95$), with no apparent systematic biases. The reaction temperature appeared to be the most sensitive variable for predictions of measured gas yields, confirming the previous results of Johansen et al. [18, 67]. The importance of the reaction temperature for predicting gas yields may be consistent with the effect of temperature on the tar reformation rate to produce syngas (or char gasification). Consistent with char gasification explanation, the temperature exponents (D_5 and E_5 ,

in models 4-5, respectively) were always positive for gases and negative for the char.

Although the overall trends of the model predictions are in general agreement with the experimental data, none of the models are complete nor do they replicate data with perfect fidelity. Experimental error must account for some of the discrepancy between the model predictions and experimental data. For gases, inaccuracies in the calibration of the micro GC can explain discrepancies as great as 3%. The char yield is determined gravimetrically, with measurement uncertainties contributing as much as 5% to the discrepancies between model predictions and measured values. In terms of the models themselves, some of the discrepancies might be attributed to the interactions between alkali metals, gas products and carbonaceous char matrix that were not considered explicitly. Moreover, the model lignocellulosic compounds were obtained from commercial suppliers and the chemical structures of the three components used in this study are not identical to their forms in biomass, potentially leading to inaccurate predictions. That stated, of the three main biomass constituents, lignin composition is most source dependent [36] and the results obtained in the model compound study suggest that the behavior of different lignin types is not strongly source dependent. Similarly, the influence of extractives and proteins were not considered, and these might modestly influence predictions.

Finally, the effects of heat and mass transfer on char and gas yields were not explicitly included in any of the models; explicitly including transport effects might improve model accuracy, as suggested originally by Yu et al. [36]. Figures S-3-S-5 provides data on the particle size, internal porosity, and

channels in particles of **xylan** and lignin used in this study, suggesting that the rates of reactive gas transport through the porous structure may need to be considered in high fidelity models which account for secondary reactions. As such, the physical properties of lignocellulosic compounds might also have a strong influence on the quantitative discrepancy, as proposed by Yu et al. [36].

4. Conclusion

This work presents yield and gas composition data for isolated lignocellulosic compounds and whole biomass reacted in a drop tube reactor operating in the temperature range from 800 to 1250°C. Reaction of lignin derived from two different sources (softwood and wheat straw) resulted in greater soot yields than cellulose and xylan, consistent with the aromatic content of lignin. No char yield was observed in cellulose pyrolysis, whereas the char yield decreased with the heat treatment temperature in pyrolysis of lignin and xylan. The influence of residence time on the char yield was less than the heat treatment temperature. Simultaneous reduction of tar and soot was achieved by impregnation of lignin from wheat straw with aqueous KNO_3 solution, leading to reduction of light hydrocarbons and carbon monoxide and increase in carbon dioxide in the syngas. Attempts to develop empirical models to explain these results showed that simple models can be used for the prediction of gaseous and char yields of natural biomass pyrolysis when terms are included for xylan, cellulose, lignin, and ash content of the fuel. Including reaction temperature further improves model accuracy, especially

for gas yields. **In future work, the authors recommend extending the model by separating the effects of primary and secondary reactions, and including explicit heat and mass transfer effects.**

Acknowledgements

The authors gratefully acknowledge financial support from the Kempe Foundation. The U.S. National Science Foundation (#1605916) funded WPI's contribution.

References

- [1] Umeki K, Yamamoto K, Namioka T, Yoshikawa K, High temperature steam-only gasification of woody biomass, *Appl Energy* 87 (2010) 791–8.
- [2] Andersson J, Lundgren J, Techno-economic analysis of ammonia production via integrated biomass gasification, *Appl Energy* 130 (2014) 484–90.
- [3] Maity SK, Opportunities, recent trends and challenges of integrated biorefinery: Part II, *Renew Sustain Energy Rev* 43 (2015) 1446–66.
- [4] Trubetskaya A, Souihi N, Umeki K, Categorization of tars from fast pyrolysis of pure lignocellulosic compounds at high temperature, *Renew Energy* 141 (2019) 751–9.
- [5] Trubetskaya A, Jensen PA, Jensen AD, Garcia Llamas AD, Umeki K, Glarborg P, Effect of fast pyrolysis conditions on biomass solid residues at high temperatures, *Fuel Process Technol* 143 (2016) 118–29.
- [6] Miller RS, Bellan J, A Generalized Biomass Pyrolysis Model Based a Superimposed Cellulose, Hemicellulose and Lignin Kinetics, *Combust Sci Tech* 126 (1-6) (1997) 97–137.
- [7] Yang H, Yan R, Chen H, Zheng C, Le DH, Liang DT, In-Depth Investigation of Biomass Pyrolysis Based on Three Major Components: Hemicellulose, Cellulose and Lignin, *Energy Fuels* 20 (2006) 388–93.

- [8] Zhou J, Chen Q, Zhao H, Cao X, Mei Q, Luo Z and etc., Biomass-oxygen gasification in a high-temperature entrained-flow gasifier, *Biotechnol Adv* 27 (5) (2009) 606–11.
- [9] Göktepe B, *Entrained Flow Gasification of Biomass*. PhD thesis, Luleå University of Technology, 2015.
- [10] Septien S, Valin S, Peyrot M, Dupont C, Salvador S, Characterization of char and soot from millimetric wood particles pyrolysis in a drop tube reactor between 800°C and 1400°C, *Fuel* 121 (2014) 216–24.
- [11] Umeki K, Moilanen A, Gomez-Barea A, Konttinen J, A model of biomass char gasification describing the change in catalytic activity of ash, *Chem Eng J* 207-208 (2012) 616–24.
- [12] Thurner F, Mann U, Kinetic Investigation of Wood Pyrolysis, *Ind Eng Chem Process Des Dev* 20 (3) (1981) 482–8.
- [13] Koufopoulos CA, Maschio G, Lucchesi A, Kinetic Modelling of the Pyrolysis of Biomass and Biomass Components, *Can J Chem Eng* 67 (1) (1989) 75–84.
- [14] Grønli MG, *A Theoretical and Experimental Study of the Thermal Degradation of Biomass*. PhD thesis, Norwegian University of Science and Technology, 1996.
- [15] Bellais M, *Modelling of the pyrolysis of large wood particles*. PhD thesis, KTH Royal Institute of Technology, 2007.

- [16] Neves D, Thunman H, Matos A, Tarelho L, Gomez-Barea A, Characterization and prediction of biomass pyrolysis products, *Prog Energy Combust Sci* 37 (2011) 611–30.
- [17] Umeki K, Kirtania K, Chen L, Bhattacharya S, Fuel Particle Conversion of Pulverized Biomass during Pyrolysis in an Entrained Flow Reactor, *Ind Eng Chem Res* 51 (2012) 13973–9.
- [18] Johansen JM, Jensen PA, Glarborg P, De Martini N, El Paul, Mitchell RE and etc., Devolatilization of Woody Biomass at Short Residence Times and High Heating Rates and Peak Temperatures, *Appl Energy* 162 (2016) 245–56.
- [19] Trubetskaya A, Surup G, Shapiro A, Bates RB, Modeling the influence of potassium content and heating rate on biomass pyrolysis, *Appl Energy* 194 (2017) 199–211.
- [20] Leth-Espensen A, Glarborg P, Jensen PA, Predicting Biomass Char Yield from High Heating Rate Devolatilization Using Chemometrics, *Energy Fuels* 32 (9) (2018) 9572–80.
- [21] Trubetskaya A, Brown A, Tompsett GA, Timko MT, Kling J, Umeki K and etc., Characterization and reactivity of soot from fast pyrolysis of lignocellulosic compounds and monolignols, *Appl Energy* 212 (2018) 1489–1500.
- [22] Couhert C, Commandre JM, Salvador S, Failure of the component additivity rule to predict gas yields of biomass in flash pyrolysis at 950°C, *Biomass Bioenergy* 33 (2009) 316–26.

- [23] Couhert C, Commandre JM, Salvador S, Is it possible to predict gas yields of any biomass after rapid pyrolysis at high temperature from its composition in cellulose, hemicellulose and lignin?, *Fuel* 88 (2009) 408–17.
- [24] Trubetskaya A, Jensen PA, Jensen AD, Steibel M, Spliethoff H, Glarborg P, Influence of fast pyrolysis conditions on yield and structural transformation of biomass char, *Fuel Process Technol* 140 (2015) 205–14.
- [25] Bouraoui Z, Dupont C, Jeguirim M, Limousy L, Gadiou R, CO₂ gasification of woody biomass chars: The influence of K and Si on char reactivity, *C R Chimie* 19 (4) (2016) 457–65.
- [26] dos Santos PSB, de Cademartori PHG, Prado R, Gatto DA, Labidi J, Composition and structure of organosolv lignins from four eucalypt species, *Wood Sci Tech* 48 (4) (2014) 873–85.
- [27] Ghaffar SH, Fan M, Structural analysis for lignin characteristics in biomass straw, *Biomass Bioenergy* 57 (2013) 264–79.
- [28] Bach-Oller A, Kirtania K, Furusjö E, Umeki K, Co-gasification of black liquor and pyrolysis oil at high temperature: Part 2. Fuel conversion, *Fuel* 197 (2017) 240–7.
- [29] Umeki K, Kirtania K, Bach-Oller A, Furusjö E, Häggström G, Reduction of Tar and Soot Formation from Entrained-Flow Gasification of Woody Biomass by Alkali Impregnation, *Energy Fuels* 31 (5) (2017) 5104–10.

- [30] Li M, Pu Y, Ragauskas AJ, Current Understanding of the Correlation of Lignin Structure with Biomass Recalcitrance, *Front Chem* 4 (45) (2016) 1–8.
- [31] Schutyser W, Renders T, Van den Bosch S, Koelewijn SF, Beckham GT, Sels BF, Chemicals from lignin: an interplay of lignocellulose fractionation, depolymerisation, and upgrading, *Chem Soc Rev* 47 (3) (2018) 852–908.
- [32] Nitsos C, Rova U, Christakopoulos P, Organosolv Fractionation of Softwood Biomass for Biofuel and Biorefinery Applications, *Energies* 11 (50) (2018) 1–23.
- [33] Cabrera Y, Cabrera A, Hofmann Larsen F, Felby C, Solid-state ^{29}Si NMR and FTIR analyses of lignin-silica coprecipitates, *Holzforschung* 70 (8) (2016) 1–20.
- [34] Tian D, Chandra RP, Lee JS, Lu C, Saddler JN, A comparison of various lignin-extraction methods to enhance the accessibility and ease of enzymatic hydrolysis of the cellulosic component of steam-pretreated poplar, *Biotechnol Biofuels* 10 (157) (2017) 1–10.
- [35] Klett AS, Purification, Fractionation, and Characterization of Lignin from Kraft Black Liquor for Use as a Renewable Biomaterial. PhD thesis, Clemson University, 2017.
- [36] Yu J, Paterson N, Blamey J, Millan M, Cellulose, xylan and lignin interactions during pyrolysis of lignocellulosic biomass, *Fuel* 191 (2017) 140–9.

- [37] Zhou H, Wu C, Onwudili JA, Meng A, Zhang Y, Williams PT, Polycyclic aromatic hydrocarbons PAH formation from the pyrolysis of different municipal solid waste fractions, *Waste Manage* 36 (2015) 136–46.
- [38] Bassilakis R, Carangelo RM, Wojtowicz MA, TG-FTIR analysis of biomass pyrolysis, *Fuel* 80 (2001) 1765–86.
- [39] Yang H, Yan R, Chen H, Lee DH, Zhang C, Characteristics of hemicellulose, cellulose and lignin pyrolysis, *Fuel* 86 (2007) 1781–8.
- [40] Yoon HC, Pozivil P, Steinfeld A, Thermogravimetric pyrolysis and gasification of lignocellulosic biomass and kinetic summative law for parallel reactions with cellulose, xylan, and lignin, *Energy Fuels* 26 (2012) 357–64.
- [41] Zhou H, Long Y, Meng A, Li Q, Zhang Y, The pyrolysis simulation of five biomass species by hemicellulose, cellulose and lignin based on thermogravimetric curves, *Thermochim Acta* 566 (2013) 36–43.
- [42] Wu C, Wang Z, Huang J, Williams PT, Pyrolysis/gasification of cellulose, hemicellulose and lignin for hydrogen production in the presence of various nickel-based catalysts, *Fuel* 106 (2013) 697–706.
- [43] Lanza R, Nogare DD, Canu P, Gas Phase Chemistry in Cellulose Fast Pyrolysis, *Ind Eng Chem Res* 48 (2009) 1391–9.
- [44] Williams A, Jones JM, Ma L, Pourkashanian M, Pollutants from the combustion of solid biomass fuels, *Prog Energy Combust Sci* 38 (2012) 113–37.

- [45] Trubetskaya A, Jensen PA, Jensen AD, Garcia Llamas AD, Umeki K, Gardini D and etc., Effects of several types of biomass fuels on the yield, nanostructure and reactivity of soot from fast pyrolysis at high temperatures, *Appl Energy* 171 (2016) 468–82.
- [46] Evans RJ, Milne TA, Molecular characterization of the pyrolysis of biomass. I. Fundamentals, *Energy Fuels* 1 (2) (1987) 123–37.
- [47] Dufour A, Weng J, Jia L, Tang X, Sirjean B, Fournet R, Revealing the chemistry of biomass pyrolysis by means of tunable synchrotron photoionisation-mass spectrometry, *RSC Advances* 3 (2013) 4786–92.
- [48] Daily JW, Jarvis MW, Gaston KR, James FW, Nimlos MR, Donohoe BS et al., Elucidation of Biomass Pyrolysis Products Using a Laminar Entrained Flow Reactor and Char Particle Imaging, *Energy Fuels* 25 (2011) 324–36.
- [49] Shin EJ, Nimlos MR, Evans RJ, The formation of aromatics from the gas-phase pyrolysis of stigmasterol: kinetics, *Fuel* 80 (12) (2001) 1681–7.
- [50] Vasiliou AK, Kim JH, Ormond TK, Piech KM, Urness KN, Scheer AM and etc., Biomass pyrolysis: thermal decomposition mechanisms of furfural and benzaldehyde, *J Chem Phys* 139 (10) (2013) 1–10.
- [51] Simoneit BRT, Schauer JJ, Nolte CG, Oros DR, Elias VO, Fraser MP and etc., Levoglucosan, a tracer for cellulose in biomass burning and atmospheric particles, *Atmos Environ* 33 (1999) 173–82.

- [52] Ross AB, Junyapoon S, Jones JM, Williams A, Bartle KD, A study of different soots using pyrolysis-GC-MS and comparison with solvent extractable material, *J Anal Appl Pyrolysis* 74 (2005) 494–501.
- [53] Zaror CA, Hutchings IS, Pyle DL, Stiles HN, Kandiyoti R, Secondary char formation in the catalytic pyrolysis of biomass, *Fuel* 64 (1985) 990–94.
- [54] Solomon PR, Best PE, Yu ZZ, Charpenay S, An Empirical Model for Coal Fluidity Based on a Macromolecular Network Pyrolysis Model, *Energy Fuels* 6 (1992) 143–54.
- [55] Hajaligol MR, Howard JB, Longwell JP, Peters WA, Product Compositions and Kinetics for Rapid Pyrolysis of Cellulose, *Ind Eng Chem Process Des Dev* 21 (1982) 457–65.
- [56] Hajaligol MR, Howard JB, Peters WA, An Experimental and Modeling Study of Pressure Effects on Tar Release by Rapid Pyrolysis of Cellulose Sheets in a Screen Heater, *Combust Flame* 95 (1993) 47–60.
- [57] DeGroot WF, Shafizadeh F, The influence of exchangeable cations on the carbonization of biomass, *J Anal Appl Pyrolysis* 6 (1984) 217–32.
- [58] Tian L, Koshland CP, Yano J, Yachandra VK, Yu ITS, Lee SC et al., Carbon-Centered Free Radicals in Particulate Matter Emissions from Wood and Coal Combustion, *Energy Fuels* 23 (5) (2009) 2523–6.
- [59] Trubetskaya A, Jensen PA, Jensen AD, Glarborg P, Hofmann Larsen F, Larsen Andersen M, Characterization of free radicals by electron spin

resonance spectroscopy in biochars from pyrolysis at high heating rates and at high temperatures, *Biomass Bioenergy* 94 (2016) 117–29.

- [60] Wood BJ, Sancier KM, Sheridan DR, Chan BL, Wise H, The mechanism of catalytic gasification of coal char. Morgantown (WV): US Department of Energy; 1981 December Report No. DE82-009461. Contract No.: DE-AC21-80-MC14593 .
- [61] Gilman JW, Lomakin S, Kashiwagi T, Vanderhart DL, Nagy V, Characterization of Flame-retarded Polymer Combustion Chars by Solid-State ^{13}C and ^{29}Si NMR and EPR, *Fire Mater* 22 (1998) 61–7.
- [62] Sancier KM, Effects of Catalysts and CO_2 Gasification on the ESR of Carbon Black II, *Preprints of Papers ACS Div Fuel Chem* 28 (1983) 62–70.
- [63] Butt DAE, Formation of phenols from the low-temperature fast pyrolysis of Radiata pine (*Pinus radiata*) - Part I. Influence of molecular oxygen, *J Anal Appl Pyrolysis* 76 (2006) 38–47.
- [64] Marsh H, The effects of impregnation of coal by alkali salts upon carbonization properties, *Fuel Process Tech* 2 (1979) 61–75.
- [65] Qu T, Guo W, Shen L, Zhao K, Experimental Study of Biomass Pyrolysis Based on Three Major Components: Hemicellulose, Cellulose, and Lignin, *Ind Eng Chem Res* 50 (2011) 10424–33.
- [66] Akaike H, Information theory and an extension of the maximum likelihood principle, Springer (1998) 199–213.

- [67] Johansen JM, Jensen PA, Glarborg P, De Martini N, El Paul, Mitchell RE, High Heating Rate Devolatilization Kinetics of Pulverized Biomass Fuels, *Energy Fuels* 32 (12) (2018) 12955–61.